NANO LETTERS

pubs.acs.org/NanoLett
Letter

Far-Field Petahertz Sampling of Plasmonic Fields

Kai-Fu Wong,[¶] Weiwei Li,[¶] Zilong Wang, Vincent Wanie, Erik Månsson, Dominik Hoeing, Johannes Blöchl, Thomas Nubbemeyer, Abdallah Azzeer, Andrea Trabattoni, Holger Lange,* Francesca Calegari,* and Matthias F. Kling*

Cite This: *Nano Lett.* 2024, 24, 5506−5512

ABSTRACT: The response of metal nanostructures to optical excitation leads to localized surface plasmon (LSP) generation with nanoscale field confinement driving applications in, for example, quantum optics and nanophotonics. Field sampling in the terahertz domain has had a tremendous impact on the ability to trace such collective excitations. Here, we extend such capabilities and introduce direct sampling of LSPs in a more relevant petahertz domain. The method allows to measure the LSP field in arbitrary nanostructures with subcycle precision. We demonstrate the technique for colloidal nanoparticles and compare the results to finite-difference time-domain calculations, which show that the build-up and dephasing of the plasmonic excitation can be resolved. Furthermore, we observe a reshaping of the spectral phase of the few-cycle pulse, and we demonstrate ad-hoc pulse shaping by tailoring the plasmonic sample. The methodology can be extended to single nanosystems and applied in exploring subcycle, attosecond phenomena.

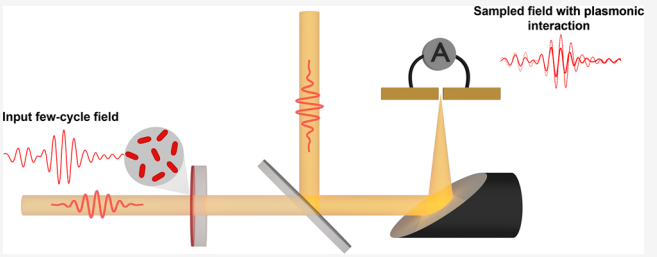

KEYWORDS: *plasmonics, plasmon dynamics, gold nanoparticles, petahertz field sampling*

INTRODUCTION

In metallic nanoparticles (NPs), the light electric field can drive the conduction band electrons into a collective oscillation on the nanoscale, referred to as localized surface plasmon (LSP).[1] Coupling of light to an LSP resonance leads to the local enhancement of the electromagnetic field and to the confinement of the light-matter interaction on the nanoscale, therefore enabling a manifold of applications including surface enhanced spectroscopy,[2] enhanced luminescence,[3] strong-field driven nanoscale currents,[4] enhanced nonlinear optical effects,[5] and strong-coupling quantum optics.[6,7] However, a direct characterization method for the electric fields emerging from the resonantly excited nanostructure is still lacking.

Subsequent to its coherent driving by the light field, Landau damping, electron−electron, electron−phonon, and electron−surface scattering result in an ultrafast (about 10 fs) plasmon decay with the energy transferred to highly excited, non-equilibrium carriers.[8−13] These hot carriers can contribute to chemical transformations on the NP surface, intensely studied in the field of heterogeneous catalysis.[14] The details of the plasmon decay channels have only been deduced from theory and dependencies on material parameters and e.g. excitation conditions have not yet been experimentally confirmed in a direct manner.[15−17] For this reason, experiments enabling more direct access to the plasmon decay of different NP systems are of strong interest. Measurements in the time domain that enable a more direct access to the plasmonic field build-up and decay of different NP systems have been accomplished with phase-retrieval methods, such as frequency-resolved optical gating.[16] These methods, do, however, not provide the carrier-envelope phase (i.e., an absolute field). They also tend to catastrophically fail for complex phases and too much noise. To circumvent these issues, field sampling of plasmonic nanoantennas has been recently implemented with electro-optical sampling, limiting the approach, however, to the terahertz domain.[18] The vast majority of plasmonic nanostructures discussed in the literature exhibit resonances in the visible spectral region, strongly motivating the extension to the petahertz (PHz) domain. As a first example heading in this direction, plasmonic nanoantennas have been utilized as near-field sensors to enhance the sensitivity for the reconstruction of the incident light electric field (E-field),[19] and extended to probing plasmonic fields in the near-field.[20] What is still lacking despite its high relevance,[21] is the realization of far-field sampling of short-lived collective excitations in the visible spectral region.

Received: February 5, 2024
Revised: March 21, 2024
Accepted: March 21, 2024
Published: March 26, 2024

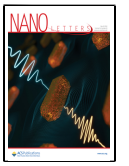

https://doi.org/10.1021/acs.nanolett.4c00658
Nano Lett. 2024, 24, 5506−5512

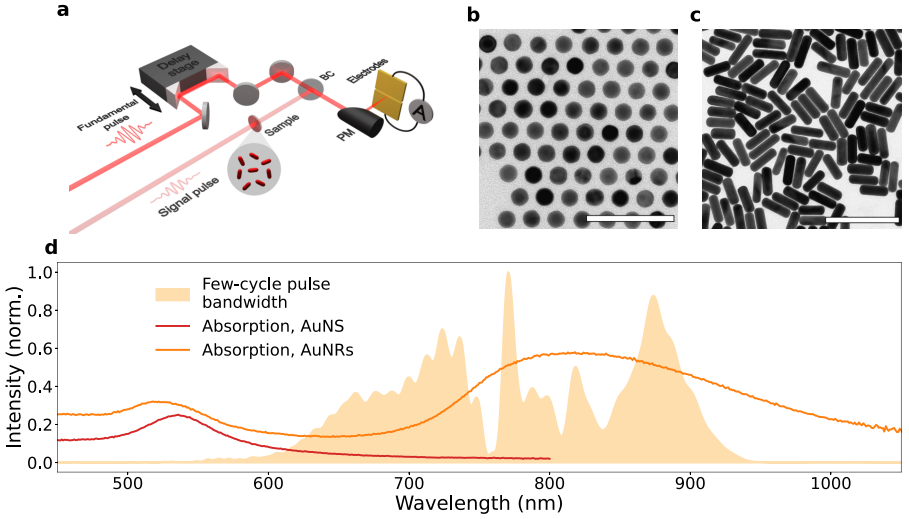

Figure 1. Experimental approach. (a) Sketch of the field sampling setup. The incident laser pulse is split into a fundamental and a signal pulse in an interferometer. The signal pulse interacts with the sample. Both pulses are recombined with variable delay and focused between two electrodes, where the TIPTOE measurement takes place. (b) TEM image of the employed AuNS with scale bar corresponding to 100 nm. (c) TEM image of the AuNRs with scale bar corresponding to 200 nm. (d) Absorption spectra of the investigated NPs (AuNS: red curve, AuNRs: orange curve) together with the incident light spectrum. BC: beam combiner, PM: parabolic mirror.

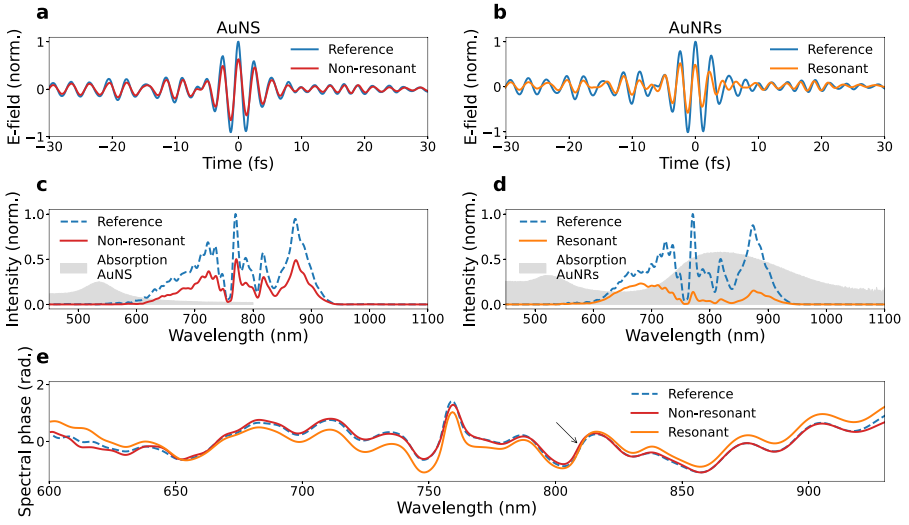

Figure 2. Optical field sampling measurements. (a) TIPTOE trace for the non-resonant AuNS. (b) TIPTOE traces for the resonant AuNRs. In both cases, the blue line depicts the TIPTOE trace of the reference (plain substrate). (c, d) Corresponding transmission spectra obtained via Fourier transform from the measurements in (a) and (b), respectively. The dashed blue curve displays the reference few-cycle spectrum. The shaded gray areas display the absorbance spectrum of the corresponding NPs. (e) Spectral phases for each case. The dashed blue line displays the reference, red the non-resonant and orange the resonant spectral phase, respectively. The black arrow indicates the crossing between the phases of the resonant and reference case.

Here, we close this gap and demonstrate sampling of few-femtosecond LSPs of colloidal NPs in the visible spectral region. Based on recent advances in methodology,[22] we implemented petahertz sampling of LSPs with the tunneling ionization with a perturbation for the time-domain observation of the electric field (TIPTOE) technique.[23] We compare the experimental data to results from finite-difference time-domain (FDTD) calculations showing that the temporal build-up and decay of the plasmon field on a few-fs time scale can be resolved. Our approach expands the tool kit for transient polarization dynamics measurements by direct field resolved (rather than intensity correlations) measurements.

Furthermore, we demonstrate extreme scale control of the transmitted fields with the NPs. With our approach we are not only sensitive to the electric field in the time domain but also directly sensitive to the phase response, which is imprinted in the phase of the sampled field. This in turn allows for the specific design of the plasmonic material to optimize the light-matter interaction for the aforementioned applications. In our case, we demonstrate the ability to shape the dispersion of ultrafast light pulses by changes of the geometry of our NPs. Our results provide a simple way of sampling plasmon fields of arbitrary nanostructures on the PHz scale and show important practical applications in the control of light fields.

RESULTS

Few-cycle pulses with a pulse duration of 4.5 fs, central wavelength of 780 nm, and repetition rate of 10 kHz were sent

https://doi.org/10.1021/acs.nanolett.4c00658
Nano Lett. 2024, 24, 5506−5512

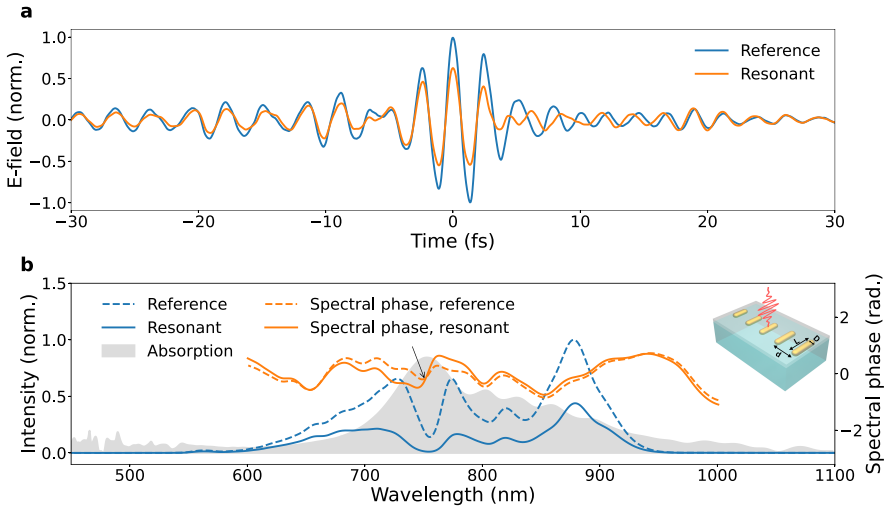

Figure 3. FDTD calculation for the resonant case. (a) Simulated E-field with the plasmonic contribution (orange) and the input pulse as experimental data (blue). (b) Retrieved spectrum (blue) and spectral phase (orange) from the FDTD calculation, displaying the transmitted E-field after propagation through the plasmonic sample. As a reference the field without sample interaction is depicted in dashed lines as well. The shaded gray area displays the absorption spectrum of the sample, in which five different sized AuNRs embedded on a fused silica matrix are used for the calculations. Insets: simulation geometry of AuNRs, with five different size dimensions considering the colloidal size distribution of the AuNRs.

into the experimental setup shown in Figure 1a. The incident light was split interferometrically into a fundamental and a signal beam. The signal beam was propagating through the plasmonic sample before being recombined with the fundamental beam for field sampling. The intensity ratio between signal and fundamental beams was chosen to be roughly 1:1000, to remain in the perturbative regime for the TIPTOE technique.[23] The peak intensities for the excitations were chosen to be under 10^{10} W/cm^2 to avoid damage of the sample, and to ensure that the interaction between the few-cycle signal pulse and the sample is in the linear regime (see Supplementary Notes 3−5 in the Supporting Information). As samples, we employed gold nanospheres (AuNS) with 20 nm diameter and gold nanorods (AuNR) with dimensions of 80 nm × 26 nm (aspect ratio of 3.1), respectively. To ensure well-defined conditions and to minimize the potential effects of plasmonic coupling, the NPs were stabilized with polymer ligands. These drive the assembly into uniform films with controlled minimal interparticle distances. Transmission electron microscopy (TEM) images of each sample are shown in Figure 1b,c. From the TEM images, we also obtained the size distributions of the colloidal samples (see Supplementary Note 1). For AuNS, the plasmon resonance only marginally overlaps with the broad bandwidth of the few-cycle near-infrared (NIR) pulse (non-resonant case), while the longitudinal surface plasmon resonance of AuNRs lies right within the NIR spectrum (resonant case); cf. Figure 1d. The samples were deposited on a fused silica substrate. A replica silica substrate was used as a reference. The dispersive contribution from the 1 mm thick fused silica substrate for the deposited NPs was carefully compensated with chirped mirrors. Observed changes should therefore arise only from the plasmon field itself. Figure 2 displays the results obtained from the TIPTOE measurements for both the non-resonant and resonant cases in the time domain. As expected for a non-resonant sample, the TIPTOE measurement performed for AuNS shown in Figure 2a exhibits a very similar E-field as the reference field with a small attenuation that can be attributed to intraband transitions in gold. This also results in almost identical spectral amplitudes and spectral phases between the sample and bare substrate as shown in Figure 2c and e, respectively. Note that the non-resonant case serves as a benchmark in our field sampling approach. In the case of AuNRs, a strong reduction in the amplitude of the E-field is observed, as expected by the resonant absorption (Figure 2d). More interestingly, the sampled E-field in the time-domain (Figure 2b) exhibits deviations from the reference: starting from the peak of the pulse envelope, we can observe a significant distortion of the optical cycles with oscillations extending in the tail of the few-cycle pulse. These distortions result in a drastic change of the spectral phase as shown in Figure 2e, which exhibits a crossing with the reference phase at the peak of the plasmon resonance around 810 nm. The phase shift due to the resonance is a well-known effect and has been reported in previous studies.[19,24] We note that we neglect CEP induced effects by the plasmonic sample itself in order to emphasize the influence of the plasmonic sample on the electric field in the time domain directly. In fact, the plasmonic sample induces a change in the CEP in the electric field itself. The field sampling technique allows tracking these changes, which we discuss further in Supplementary Note 8.

The experimental observations were compared to FDTD calculations implemented using Lumerical 2022 R1 software (ANSYS, Inc.).[25] As input parameters we used the particle dimensions, the dielectric constants of the materials, and the sampled incident E-field. To account for the inhomogeneous broadening of the plasmon resonance, we calculated the interaction between the experimental few-cycle field with five particles of different sizes, considering the determined size distribution from TEM analysis as a weighting factor. The calculation results are summarized in Figure 3.

The obtained traces for the plasmonic interaction agree with the experimental traces (Figure 3a). At 5 fs the discontinuity of the E-field is indicated, and the delayed oscillation can be observed until 12 fs. The agreement persists for the spectral phases. As in the experiment, the spectral phase between reference and plasmonic system exhibits a visible phase

https://doi.org/10.1021/acs.nanolett.4c00658
Nano Lett. 2024, 24, 5506−5512

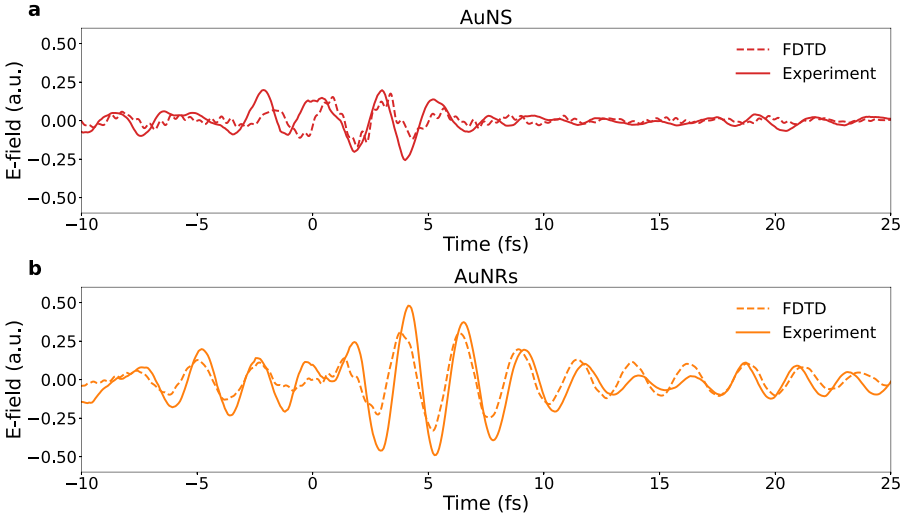

Figure 4. Sampling of plasmon fields. (a) Differential field contributions for the non-resonant AuNS with the experimental data as solid line and the FDTD data as dashed line. (b) Differential field contributions for the resonant AuNRs.

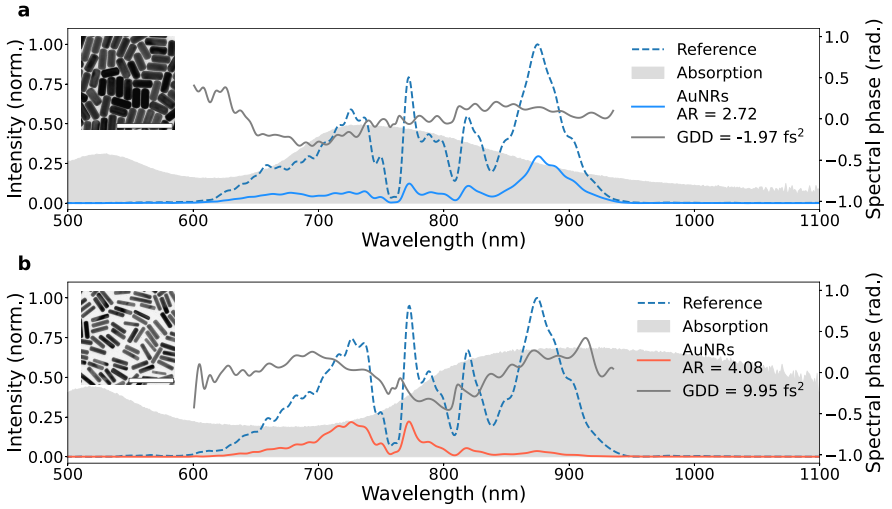

Figure 5. Comparison of the propagating pulse spectral properties for AuNRs with resonances shifted relative to the AuNRs discussed before. (a) Blue-shifted AuNRs. (b) Red-shifted AuNRs. The absorption position of the plasmonic resonances are hinted as shaded gray area.The residual spectral phase contribution with its extracted GDD value is depicted as the gray line in each case. Exemplary TEM images of the AuNR samples with corresponding scale bars of 200 nm each are shown as insets.

crossing at the central resonance around 750 nm in this case, cf. Figure 3b (indicated by the arrow).

To resolve the onset of the plasmonic excitation from the time-resolved measurements, we subtracted the TIPTOE traces between the sample and the reference. In this way, we isolate the contribution of the plasmon from the driving few-cycle field in the far-field domain. The results are reported in Figure 4.

For the non-resonant case, the differential signal is almost negligible. For the resonant case, a clear buildup of an additional field component can be resolved, with a subsequent decay with a lifetime in the order of 10 fs, after which the differential field approaches the baseline. Treating the calculated data the same way, we observed a qualitative agreement with the experiment. The plasmon drive is well reproduced by the simulations, while we experimentally observe a faster decay, which could be attributed to inhomogeneous broadening due to plasmon coupling and increased damping at elevated temperatures.[26,27] The visible ultrafast decay can be attributed to the ultrafast dephasing time of the plasmon, which conversely to previous measurements[19] can now be retrieved from far-field measurements (see Supplementary Note 7). The pulse interaction with the plasmon is also reflected in the optical dispersion. Applying a polynomial fit to extract the group delay dispersion (GDD) yields different values for the plasmonic interaction compared with the reference sample. A positive GDD enhancement of approximately 8.03 fs^2 compared to the original phase value was observed after propagation through the resonant AuNRs sample. The enhancement was consistent with differently chirped pulses (S2 of Supplement 1). Interestingly, we observe that the residual spectral phase, representing the plasmonic contribution, displays a positive parabolic shape close to the peak of the plasmon resonance. In contrast, the non-resonant AuNS induce no significant change of the dispersion. To further explore this effect, we performed measurements with samples displaying different plasmon resonances by altering the aspect ratio (AR) of the AuNRs. As samples we used AuNRs

https://doi.org/10.1021/acs.nanolett.4c00658
Nano Lett. 2024, 24, 5506−5512

with dimensions of 71 × 26 and 78 × 19 nm corresponding to an AR of 2.7 and 4.1 respectively. As the AR for AuNRs changes, the longitudinal plasmon resonance shifts in frequency. We observe that the spectral phase of the few-cycle pulse is altered correspondingly; cf. Figure 5.

As the plasmon absorption shifts relative to the previous resonant case, we also observe a shift of the positive parabolic contribution. In particular, for the plasmon resonance overlapping with the blue part of the spectrum, the minimum of the parabola shifts toward the blue, and correspondingly the remaining spectral phase exhibits a slightly negative parabolic shape that results in a negative GDD. In contrast, for the plasmon resonance overlapping with the red part of the spectrum, the minimum of the parabola shifts toward the red and results in an increase of the positive GDD. Tailoring of the plasmonic resonance is straightforward by changing the properties of the NP such as shape, size, or environment and thus allows the realization of ad-hoc pulse shaping. Moreover, the ability to tailor plasmon resonances with a broad bandwidth facilitates the possibility of manipulating the spectral properties of broadband few-optical-cycle pulses. This concept was already anticipated in a theoretical study proposing the use of plasmonic NPs as metasurfaces to engineer ultrashort pulses[28] and it has been experimentally demonstrated with 45 fs long pulses.[29] In this context, our approach demonstrates the feasibility of shaping broadband few-cycle pulses by using broad plasmon resonances.

CONCLUSION

We demonstrated the direct sampling of few-femtosecond localized surface plasmons at near-infrared to visible wavelengths, which are the most relevant in nanoplasmonics. The method provides the absolute field in the petahertz domain. We demonstrated the approach by measuring the build up and dephasing of localized surface plasmons of colloidal gold nanostructures. The methodology can be straightforwardly extended to single nanostructures using a microscopic setup, as well as to dense NP structures to explore coupling effects. The ability to resolve absolute plasmonic fields with subcycle, attosecond resolution, opens an avenue to study strong-field plasmonics. Furthermore, we demonstrated that the broadband plasmon resonance of nanostructures can alter the optical properties of few-cycle pulses. The field sampling allows for direct extraction of the spectral phase without the application of any reconstruction algorithms. With careful design of such plasmonic nanostructures, their usage for shaping of ultrashort laser pulses becomes in principle feasible.

METHODS

Sample Preparation. Monocrystalline NPs with uniform size distribution were synthesized via established wet-chemistry approaches, namely, the *seed-mediated growth* approach. The detailed protocol for the synthesis of AuNS is stated in refs.[30,31] The protocol for AuNRs is stated in ref.[32] To prepare the NPs for the optical experiment, in a first step the hexadecyltrimethylammonium chloride (CTAC)/hexadecyltrimethylammonium bromide (CTAB) stabilized particles in aqueous solution were transferred to an organic solution (toluene), in which the particles are stabilized by thiol-terminated polystyrene (PSSH) with a molar weight of 25k g/mol. The PSSH facilitates a uniform NP distribution and ensures a minimum interparticle distance. The reaction was carried out in 1 mL of tetrahydrofuran (THF), where the solution was stirred for three min in a glass vial. By shaking the vial after the reaction, a thick product stuck at the side of the vial, with the remaining supernatant on the bottom, which was removed. The remaining product in the vial was treated under a nitrogen atmosphere to dry the sample and was then redispersed with toluene. After three washing steps via centrifugation (10k g, 20 min each washing step) with toluene in which 0.1 M PSSH was dispersed, the 25 μL of the particle solution were spin-coated onto the plasma cleaned silica substrate (EKSMA Optics) at low spin speeds (100 rpms) until the organic solution evaporated completely. Materials: CTAB and CTAC were purchased from Sigma-Aldrich (USA), thiol-terminated PSSH was purchased from Polymer Source (Canada), THF (>99.5%) was purchased from VWR Chemicals (USA) and toluene (>99.8%) was purchased from Thermo Fisher Scientific (USA).

Characterization of Samples. For the as-synthesized particles, the characterization was carried out via UV/vis absorption spectroscopy and transmission electron microscopy (TEM). Absorption spectra were recorded by using a Varian Cary 50 spectrometer. For TEM analysis, a droplet of AuNS or AuNP solution was deposited on amorphous carbon-coated copper grids. The grids were dried in air overnight to remove residual solvent. TEM images were obtained using a JEOL JEM-1011 transmission electron microscope operating at 100 kV. The particles displayed a narrow size distribution, which was determined based on the width of the plasmon absorption and the TEM data. The deposited NPs were characterized by UV/vis-absorption spectroscopy. For the NPs on the substrate, a slight red-shift and broadening can be observed, one possible source originating from plasmon coupling. This would most likely lead to faster damping of the plasmon oscillation. Further effects that play a role in the broadening could be changes of the environment. Nonetheless, the assumption that the observed plasmon response mainly displays the properties of the individual particles is valid, as the shift is not too pronounced.

ASSOCIATED CONTENT

Data Availability Statement

Data underlying the results presented in this paper are not publicly available at this time but may be obtained from the authors upon reasonable request.

Supporting Information

The Supporting Information is available free of charge at https://pubs.acs.org/doi/10.1021/acs.nanolett.4c00658.

Size characterization of colloidal NPs, pulse characterization including dispersion characteristics, detailed experimental setup, linear-response calibration, damage threshold evalulation, basic concept of data analysis, additions and details of FDTD simulations, time-frequency analysis (PDF)

AUTHOR INFORMATION

Corresponding Authors

Holger Lange − *The Hamburg Centre for Ultrafast Imaging, 22761 Hamburg, Germany; Intitute of Physics and Astronomy, Universität Potsdam, 14476 Potsdam, Germany;* orcid.org/0000-0002-4236-2806; Email: holger.lange@uni-hamburg.de

https://doi.org/10.1021/acs.nanolett.4c00658
Nano Lett. 2024, 24, 5506−5512

Francesca Calegari − *The Hamburg Centre for Ultrafast Imaging, 22761 Hamburg, Germany; Center for Free-Electron Laser Science CFEL, Deutsches Elektronen-Synchrotron DESY, 22607 Hamburg, Germany*; Email: francesca.calegari@desy.de

Matthias F. Kling − *Max Planck Institute of Quantum Optics, 85478 Garching, Germany; Physics Department, Ludwig-Maximilians-Universität Munich, 85748 Garching, Germany; Stanford PULSE Institute, SLAC National Accelerator Laboratory, Menlo Park, California 94025, United States; Applied Physics Department, Stanford University, Stanford, California 94305, United States*; orcid.org/0000-0002-1710-0775; Email: kling@stanford.edu

Authors

Kai-Fu Wong − *The Hamburg Centre for Ultrafast Imaging, 22761 Hamburg, Germany; Center for Free-Electron Laser Science CFEL, Deutsches Elektronen-Synchrotron DESY, 22607 Hamburg, Germany*; orcid.org/0009-0007-0133-8723

Weiwei Li − *Max Planck Institute of Quantum Optics, 85478 Garching, Germany; Physics Department, Ludwig-Maximilians-Universität Munich, 85748 Garching, Germany*

Zilong Wang − *Max Planck Institute of Quantum Optics, 85478 Garching, Germany; Physics Department, Ludwig-Maximilians-Universität Munich, 85748 Garching, Germany*

Vincent Wanie − *Center for Free-Electron Laser Science CFEL, Deutsches Elektronen-Synchrotron DESY, 22607 Hamburg, Germany*; orcid.org/0000-0001-8274-4617

Erik Månsson − *Center for Free-Electron Laser Science CFEL, Deutsches Elektronen-Synchrotron DESY, 22607 Hamburg, Germany*; orcid.org/0000-0003-3567-2985

Dominik Hoeing − *The Hamburg Centre for Ultrafast Imaging, 22761 Hamburg, Germany*; orcid.org/0000-0002-3965-0903

Johannes Blöchl − *Max Planck Institute of Quantum Optics, 85478 Garching, Germany; Physics Department, Ludwig-Maximilians-Universität Munich, 85748 Garching, Germany*; orcid.org/0000-0003-3667-2872

Thomas Nubbemeyer − *Max Planck Institute of Quantum Optics, 85478 Garching, Germany; Physics Department, Ludwig-Maximilians-Universität Munich, 85748 Garching, Germany*

Abdallah Azzeer − *Attosecond Science Laboratory, Physics and Astronomy Department, King-Saud University, Riyadh 11451, Saudi Arabia*

Andrea Trabattoni − *Center for Free-Electron Laser Science CFEL, Deutsches Elektronen-Synchrotron DESY, 22607 Hamburg, Germany; Institute of Quantum Optics, Leibniz Universität Hannover, 30167 Hannover, Germany*

Complete contact information is available at: https://pubs.acs.org/10.1021/acs.nanolett.4c00658

Author Contributions

¶K.W. and W.L. contributed equally to this work.

Author Contributions

M.F.K. and F.C. conceived the research project and designed the experiment with H.L.; D.H. and H.L. developed the samples. K.W. and W.L. performed the experiments under guidance of Z.W. A.A. was involved in the original design of the field sampling setup. W.L. and Z.W. performed the FDTD simulations. J.B. and T.N. supported the laser and experimental operations. V.W., E.M., and A.T. were involved in the analysis of the experimental data and assisted the preliminary characterization of the samples. K.W. and W.L. wrote the initial draft of the manuscript, on which all coauthors commented.

Notes

The authors declare no competing financial interest.

■ ACKNOWLEDGMENTS

We acknowledge fruitful discussions with Markus Raschke, Nirit Dudovich and Ferenc Krausz. This work was supported by the German Research Foundation (DFG) via the Cluster of Excellence "Advanced Imaging of Matter" (EXC 2056, 390715994). H.L. acknowledges funding by the DFG via project 432266622. K.W., H.L., and F.C. acknowledge financial support by PIER, partnership of Universität Hamburg and DESY, under project PIF-2022-08. M.F.K. is grateful for partial support by the Max Planck Society via the Max Planck Fellow program. J.B. acknowledges support by the Max Planck School of Photonics. M.F.K.'s work at SLAC is supported by the U.S. Department of Energy, Office of Science, Basic Energy Sciences under DE-AC02-76SF00515, and FWP SC0063. Z.W. acknowledges support from the Alexander von Humboldt Foundation. A.T. acknowledges support from the Helmholtz association under the Helmholtz Young Investigator Group VH-NG-1603A.A. is grateful for support by the Researchers Supporting Project RSP-2021/152, King Saud University, Riyadh, Saudi Arabia.

■ REFERENCES

(1) Maier, S. A. *Plasmonics: Fundamentals and Applications*; Springer: New York, 2007.

(2) Schlücker, S. Surface-Enhanced Raman Spectroscopy: Concepts and Chemical Applications. *Angew. Chem., Int. Ed.* **2014**, *53*, 4756−4795.

(3) Fusella, M. A.; Saramak, R.; Bushati, R.; Menon, V. M.; Weaver, M. S.; Thompson, N. J.; Brown, J. J. Plasmonic enhancement of stability and brightness in organic light-emitting devices. *Nature* **2020**, *585*, 379−382.

(4) Dombi, P.; Pápa, Z.; Vogelsang, J.; Yalunin, S. V.; Sivis, M.; Herink, G.; Schäfer, S.; Groß, P.; Ropers, C.; Lienau, C. Strong-field nano-optics. *Rev. Mod. Phys.* **2020**, *92*, 025003.

(5) Kauranen, M.; Zayats, A. V. Nonlinear plasmonics. *Nat. Photonics* **2012**, *6*, 737−748.

(6) Mueller, N. S.; Okamura, Y.; Vieira, B. G. M.; Juergensen, S.; Lange, H.; Barros, E. B.; Schulz, F.; Reich, S. Deep strong light-matter coupling in plasmonic nanoparticle crystals. *Nature* **2020**, *583*, 780−784.

(7) Bogdanov, S. I.; Boltasseva, A.; Shalaev, V. M. Overcoming quantum decoherence with plasmonics. *Science* **2019**, *364* (6440), 532−533.

(8) Wang, B.; Yu, P.; Wang, W.; Zhang, X.; Kuo, H.-C.; Xu, H.; Wang, Z. M. High-Q Plasmonic Resonances: Fundamentals and Applications. *Advanced Optical Materials* **2021**, *9*, 2001520.

(9) Li, Y.; Sun, Q.; Zu, S.; Shi, X.; Liu, Y.; Hu, X.; Ueno, K.; Gong, Q.; Misawa, H. Correlation between Near-Field Enhancement and Dephasing Time in Plasmonic Dimers. *Phys. Rev. Lett.* **2020**, *124*, 163901.

(10) Santiago, E. Y.; Besteiro, L. V.; Kong, X.-T.; Correa-Duarte, M. A.; Wang, Z.; Govorov, A. O. Efficiency of Hot-Electron Generation in Plasmonic Nanocrystals with Complex Shapes: Surface-Induced Scattering, Hot Spots, and Interband Transitions. *ACS Photonics* **2020**, *7*, 2807−2824.

(11) Besteiro, L. V.; Yu, P.; Wang, Z.; Holleitner, A. W.; Hartland, G. V.; Wiederrecht, G. P.; Govorov, A. O. The fast and the furious:

Ultrafast hot electrons in plasmonic metastructures. Size and structure matter. *Nano Today* **2019**, *27*, 120−145.
(12) Boriskina, S. V.; Cooper, T. A.; Zeng, L.; Ni, G.; Tong, J. K.; Tsurimaki, Y.; Huang, Y.; Meroueh, L.; Mahan, G.; Chen, G. Losses in plasmonics: from mitigating energy dissipation to embracing loss-enabled functionalities. *Advances in Optics and Photonics* **2017**, *9*, 775−827.
(13) Hoeing, D.; Salzwedel, R.; Worbs, L.; Zhuang, Y.; Samanta, A. K.; Lübke, J.; Estillore, A. D.; Dlugolecki, K.; Passow, C.; Erk, B.; Ekanayake, N.; Ramm, D.; Correa, J.; Papadopoulou, C. C.; Noor, A. T.; Schulz, F.; Selig, M.; Knorr, A.; Ayyer, K.; Küpper, J.; Lange, H. Time-resolved single-particle x-ray scattering reveals electron-density gradients as coherent plasmonic-nanoparticle-oscillation source. *Nano Lett.* **2023**, *23*, 5943−5950.
(14) Zhang, Y.; He, S.; Guo, W.; Hu, Y.; Huang, J.; Mulcahy, J. R.; Wei, W. D. Surface-Plasmon-Driven Hot Electron Photochemistry. *Chem. Rev.* **2018**, *118*, 2927−2954.
(15) Avalos-Ovando, O.; Besteiro, L. V.; Wang, Z.; Govorov, A. O. Temporal plasmonics: Fano and Rabi regimes in the time domain in metal nanostructures. *Nanophotonics* **2020**, *9*, 3587−3595.
(16) Anderson, A.; Deryckx, K. S.; Xu, G. X.; Steinmeyer, G.; Raschke, M. B. Few-femtosecond plasmon dephasing of a single metallic nanostructure from optical response function reconstruction by interferometric frequency resolved optical gating. *Nano Lett.* **2010**, *10*, 2519−2524.
(17) Zentgraf, T.; Christ, A.; Kuhl, J.; Giessen, H. Tailoring the ultrafast dephasing of quasiparticles in metallic photonic crystals. *Phys. Rev. Lett.* **2004**, *93*, 243901.
(18) Fischer, M. P.; Maccaferri, N.; Gallacher, K.; Frigerio, J.; Pellegrini, G.; Paul, D. J.; Isella, G.; Leitenstorfer, A.; Biagoni, P.; Brida, D. Field-resolved detection of the temporal response of a single plasmonic antenna in the mid-infrared. *Optica* **2021**, *8* (6), 898−903.
(19) Bionta, M. R.; Ritzkowsky, F.; Turchetti, M.; Yang, Y.; Mor, D. C.; Putnam, W. P.; Kaertner, F. X.; Berggren, K. K.; Keathley, P. D. On-chip sampling of optical fields with attosecond resolution. *Nat. Photonics* **2021**, *15*, 456−460.
(20) Luo, Y.; Neubrech, F.; Martin-Jimenez, A.; Liu, N.; Kern, K.; Garg, M. Real-time tracking of coherent oscillations of electrons in a nanodevice by photo-assisted tunnelling. *Nat. Commun.* **2024**, *15*, 1316.
(21) Stockman, M. I.; Kneipp, K.; Bozhevolnyi, S. I.; Saha, S.; Dutta, A.; Ndukaife, J.; Kinsey, N.; Reddy, H.; Guler, U.; Shalaev, V. M.; Boltasseva, A.; Gholipour, B.; Krishnamoorthy, H. N. S.; MacDonald, K. F.; Soci, C.; Zheludev, N. I.; Savinov, V.; Singh, R.; Groß, P.; Lienau, C.; Vadai, M.; Solomon, M. L.; Barton, D. R.; Lawrence, M.; Dionne, J. A.; Boriskina, S. V.; Esteban, R.; Aizpurua, J.; Zhang, X.; Yang, S.; Wang, D.; Wang, W.; Odom, T. W.; Accanto, N.; de Roque, P. M.; Hancu, I. M.; Piatkowski, L.; van Hulst, N. F.; Kling, M. F. Roadmap on plasmonics. *Journal of Optics* **2018**, *20* (4), 043001.
(22) Herbst, A.; Scheffter, K.; Bidhendi, M. M.; Kieker, M.; Srivastava, A.; Fattahi, H. Recent advances in petahertz electric field sampling. *Journal of Physics B: Atomic, Molecular and Optical Physics* **2022**, *55* (17), 172001.
(23) Park, S. B.; Kim, K.; Cho, W.; Hwang, S. I.; Ivanov, I.; Nam, C. H.; Kim, K. T. Direct sampling of a light wave in air. *Optica* **2018**, *5* (4), 402−408.
(24) Yu, N.; Genevet, P.; Kats, M. A.; Aieta, F.; Tetienne, J. P.; Capasso, F.; Gaburro, Z. Light propagation with phase discontinuities: Generalized laws of reflection and refraction. *Science* **2011**, *334*, 333−337.
(25) Alsayed, A. E.; Ghanim, A. M.; Yahia, A.; Swillam, M. A. Giant localized electromagnetic field of highly doped silicon plasmonic nanoantennas. *Sci. Rep.* **2023**, *13* (1), 5793.
(26) Brown, A. M.; Sundararaman, R.; Narang, P.; Goddard, W. A. I.; Atwater, H. A. Nonradiative Plasmon Decay and Hot Carrier Dynamics: Effects of Phonons, Surfaces, and Geometry. *ACS Nano* **2016**, *10*, 957−966.
(27) Harutyunyan, H.; Martinson, A. B. F.; Rosenmann, D.; Khorashad, L. K.; Besteiro, L. V.; Govorov, A. O.; Wiederrecht, G. P. Anomalous ultrafast dynamics of hot plasmonic electrons in nanostructures with hot spots. *Nat. Nanotechnol.* **2015**, *10*, 770−774.
(28) Rahimi, E.; Sendur, K. Femtosecond pulse shaping by ultrathin plasmonic metasurfaces. *J. Opt. Soc. Am. B* **2016**, *33* (2), A1.
(29) Geromel, R.; Georgi, P.; Protte, M.; Lei, S.; Bartley, T.; Huang, L.; Zentgraf, T. Compact metasurface-based optical pulse-shaping device. *Nano Lett.* **2023**, *23*, 3196−3201.
(30) Zheng, Y.; Zhong, X.; Li, Z.; Xia, Y. Successive, seed-mediated growth for the synthesis of single-crystal gold nanospheres with uniform diameters controlled in the range of 5−150 nm. *Part. Part. Syst. Charact.* **2014**, *31*, 266−273.
(31) Schulz, F.; Lange, H. Optimizing interparticle gaps in large-scale gold nanoparticle supercrystals for flexible light-matter coupling. *Advanced Optical Materials* **2022**, *10*, 2202064.
(32) Schulz, F.; Friedrich, W.; Hoppe, K.; Vossmeyer, T.; Weller, H.; Lange, H. Effective PEGylation of gold nanorods. *Nanoscale* **2016**, *8*, 7296−7308.

https://doi.org/10.1021/acs.nanolett.4c00658
Nano Lett. 2024, 24, 5506−5512